

**UNCLASSIFIED**

---

**AD. 296 905**

*Reproduced  
by the*

**ARMED SERVICES TECHNICAL INFORMATION AGENCY  
ARLINGTON HALL STATION  
ARLINGTON 12, VIRGINIA**



---

**UNCLASSIFIED**

NOTICE: When government or other drawings, specifications or other data are used for any purpose other than in connection with a definitely related government procurement operation, the U. S. Government thereby incurs no responsibility, nor any obligation whatsoever; and the fact that the Government may have formulated, furnished, or in any way supplied the said drawings, specifications, or other data is not to be regarded by implication or otherwise as in any manner licensing the holder or any other person or corporation, or conveying any rights or permission to manufacture, use or sell any patented invention that may in any way be related thereto.

CATALOGED BY ASTIA

AS AD NO. 296905

296 905

ADC-TDR 62-360, Vol. II

ASTIA NO.

February 1963

# Long Range Communications Interference Study Technical Note

## on Investigation of the Fresnel Region of A Cassegrain Antenna

Dougal W. S. Prins  
Contract AF30(602)-2528

Prepared for

ROME AIR DEVELOPMENT CENTER  
AIR RESEARCH AND DEVELOPMENT COMMAND  
UNITED STATES AIR FORCE  
Griffiss Air Force Base  
New York

**MELPAR**  **INC**

A SUBSIDIARY OF WESTINGHOUSE AIR BRAKE COMPANY

3000 ARLINGTON BOULEVARD

FALLS CHURCH, VIRGINIA

#### ASTIA NOTICE

Qualified requestors may obtain copies of this report from the ASTIA Document Service Center, Arlington Hall Station, Arlington 12, Virginia. ASTIA Services for the Department of Defense contractors are available through the "Field of Interest Register" on a "need-to-know" certified by the cognizant military agency of their project or contract.

RADC-TDR-62-360, Vol II  
ASTIA No.

February 1963

LONG RANGE COMMUNICATIONS  
INTERFERENCE STUDY  
TECHNICAL NOTE  
ON  
INVESTIGATION OF THE FRESNEL REGION  
OF  
A CASSEGRAIN ANTENNA

Contract AF30(602)-2528

Prepared by  
Dougal W. S. Prins  
Approved by  
Steven M. Sussman

Prepared for  
ROME AIR DEVELOPMENT CENTER  
AIR RESEARCH AND DEVELOPMENT COMMAND  
UNITED STATES AIR FORCE  
Griffiss Air Force Base  
New York

MELPAR, INC.  
APPLIED SCIENCE DIVISION  
Falls Church, Virginia

### NOTICES

ASTIA NOTICE: Qualified requestors may obtain copies of this report from the ASTIA Document Service Center, Arlington Hall Station, Arlington 12, Virginia. ASTIA Services for the Department of Defense contractors are available through the "Field of Interest Register" on a "need-to-know" certified by the cognizant military agency of their project or contract.

## FOREWORD

This report is one of four Technical Notes issued under contract AF30(602)-2528 entitled Long Range Communications Interference Study. Each Technical Note is self-contained and its contents are of a sufficiently specialized nature to permit independent circulation. A Final Report draws upon the results reported in the Technical Notes, interrelates the material, and states conclusions and recommendations.

This study was sponsored by Rome Air Development Center, Air Force Systems Command, Electromagnetic Vulnerability Laboratory. The research work and administration was under the direction of Sampson Seideman, Task Engineer.

# ABSTRACT

A theoretical and experimental investigation of the electromagnetic field in the Fresnel Region of a Cassegrain antenna was conducted. Good agreement of experiment and theory was obtained near the beam axis. The most significant off-axis radiation was found to be due to forward spillover from the sub-reflector. The magnitude of mutual coupling of two Cassegrain antennas through this forward spillover as a function of separation distance is estimated, and methods of reducing the spillover are recommended.



## TABLE OF CONTENTS

	Page
Section 1. INTRODUCTION	1
Section 2. DESCRIPTION OF MEASUREMENTS	3
Section 3. EXPERIMENTAL RESULTS	7
Section 4. THEORETICAL INVESTIGATION	19
4.1 The Fresnel Integral of the Diffraction Field "Off Axis"	19
4.2 The Fresnel Integral of the Diffraction Field "On Axis"	22
Section 5. COMPARISON OF THEORETICAL AND EXPERIMENTAL PATTERNS	25
Section 6. CONCLUSIONS AND RECOMMENDATIONS	27
BIBLIOGRAPHY	29

# LIST OF ILLUSTRATIONS

	Title	Page
Figure		
1	Cassegrain Antenna System	4
2	Side View Detail of Cassegrain Antenna System	5
3	Field Setup for Taking Measurements	6
4	$w = 68\pi$ , $12^\circ$ Azimuth Pattern	8
5	$w = 34\pi$ , $12^\circ$ Azimuth Pattern	9
6	$w = 33\pi$ , $12^\circ$ Azimuth Pattern	10
7	$w = 17\pi$ , $12^\circ$ Azimuth Pattern	11
8	$w = 3.6\pi$ , $12^\circ$ Azimuth Pattern	12
9	$w = 68\pi$ , $60^\circ$ Azimuth Pattern	13
10	$w = 34\pi$ , $60^\circ$ Azimuth Pattern	14
11	$w = 33\pi$ , $60^\circ$ Azimuth Pattern	15
12	$w = 17\pi$ , $60^\circ$ Azimuth Pattern	16
13	$w = 3.6\pi$ , $60^\circ$ Azimuth Pattern	17

## Section 1. INTRODUCTION

One of the most serious interference problems associated with the proposed global passive satellite communications system concerns the juxtaposition of a number of large aperture microwave antennas, each radiating extremely-high average power, and operating simultaneously in transmitting and receiving modes at each ground terminal site. The exact number of these antennas to be used at any given site is not presently known, but 60-foot dishes radiating 50 kw of average power in the 7.0 - 7.7 kmcps band have been proposed.(1)

GE has considered the problem of proper isolation of transmitter and receiver at the same antenna. It is, however, conceivable that transmitter power radiating from one antenna could interfere with a signal received at another antenna at the same site. Even though the number of antennas at a given site is not known, the mutual interference problem can be resolved by considering all the combinations of antennas, taken two at a time. It is this problem of coupling between two antennas which is analyzed in this Technical Note.

In any analysis of "on site" mutual interference between high-gain antennas, knowledge of the behavior of the electromagnetic field in the "Near Zone" and "Fresnel Region" is of primary importance. The boundary between the "near" or reactive component of the field and the radiating component or "optical Fresnel Region" has not been clearly established in the literature; however, the estimate of Kay(2) and Hu(3) that the reactive boundary extends several aperture diameters appears most acceptable for large antennas operating at small wavelengths.

The Fresnel Region field distribution for circular apertures has been evaluated by Hanson(4) and Hu(3) in terms of Lommel functions. Normalized field distribution curves for both amplitude and phase have been computed by Hu(3) for various aperture illuminations to a distance from the aperture where the "on axis" power density is a maximum. Hu(3) has also derived power transfer formulae expressed in terms of these field distributions.

This report describes a theoretical and experimental investigation of the electromagnetic field in the Fresnel Region of a Cassegrain antenna having structural and operating characteristics modeled to correspond with those proposed for the antennas to be used in the satellite communication system.

In the experimental program, power patterns were taken at various distances in the Fresnel Region and Near Zone of a scale model Cassegrain antenna. The theoretical investigation compares the expressions derived by Hu and others with the experimental data, and presents an interpretation of the results as a tool for the prediction of actual patterns. The limitations of the proposed antenna system with respect to on-site interference are evaluated, and methods for reducing these defects are presented.

## Section 2. DESCRIPTION OF MEASUREMENTS

A Cassegrain antenna system was developed using a parabolic dish 10 feet in diameter as a primary reflector, and a hyperboloid 22 inches in diameter made of molded fiberglass coated with reflecting paint was used as a subreflector. An optimum gain pyramidal horn designed to produce a 10 db taper for both E and H planes in conjunction with the subreflector at the scale frequency was used as the primary feed. The complete assembly is shown in Figures 1 and 2.

The proposed antenna system describes a 60-foot parabolic dish as a main reflector operating at a frequency of 7000 mc. A scale reduction of 6 to 1 for a 10-foot dish would require a frequency of 42,000 mc. Unfortunately, klystrons operating at this frequency were found to have insufficient power to perform the desired measurements; therefore a 5789 Sylvania magnetron having a peak output of 50,000 watts at 35,000 mc with a repetition rate of 1000 pps, and a pulse duration of 0.25 microseconds was used. The antenna model therefore represents a 50-foot dish operating at 7,000 mc for a scale reduction of 5 to 1, or a 60-foot dish operating at 5,883 mc for a scale reduction of 6 to 1. This limitation is not severe since consideration of the magnitude of the parameters show that the resulting amplitude distributions would differ only slightly.

The orientation of the apparatus used in the measurements is shown in Figure 3. A 24.6 db rectangular standard gain horn mounted on a movable platform, was used as the field probe. The signal from the field probe was detected with a type 618 Bolometer detector mount, frequency range 18,000 mc to 40,000 mc, waveguide mounted to the primary feed horn of the Cassegrain antenna. The detected signal was then fed to an Antlab rectangular pattern recorder, having a dynamic range of 40 db. Patterns of  $12^\circ$ ,  $60^\circ$ , and  $360^\circ$  were taken in both azimuth and elevation for vertical linear polarization at distances of 26.2, 52.4, 54, 104.8 and 496 feet. These distances were selected to correspond to normalized functions of  $w$  of  $68\pi$ ,  $34\pi$ ,  $33\pi$ ,  $17\pi$  and  $3.6\pi$  respectively where  $w = 2\pi a^2/\lambda R$ ,  $a$  = radius of the aperture,  $\lambda$  = wavelength, and  $R$  the distance from the dish. With a scale factor of 5 to 1 these distances correspond to 131, 262, 270, 524 and 2480 feet respectively for the full-scale antenna system being modeled.

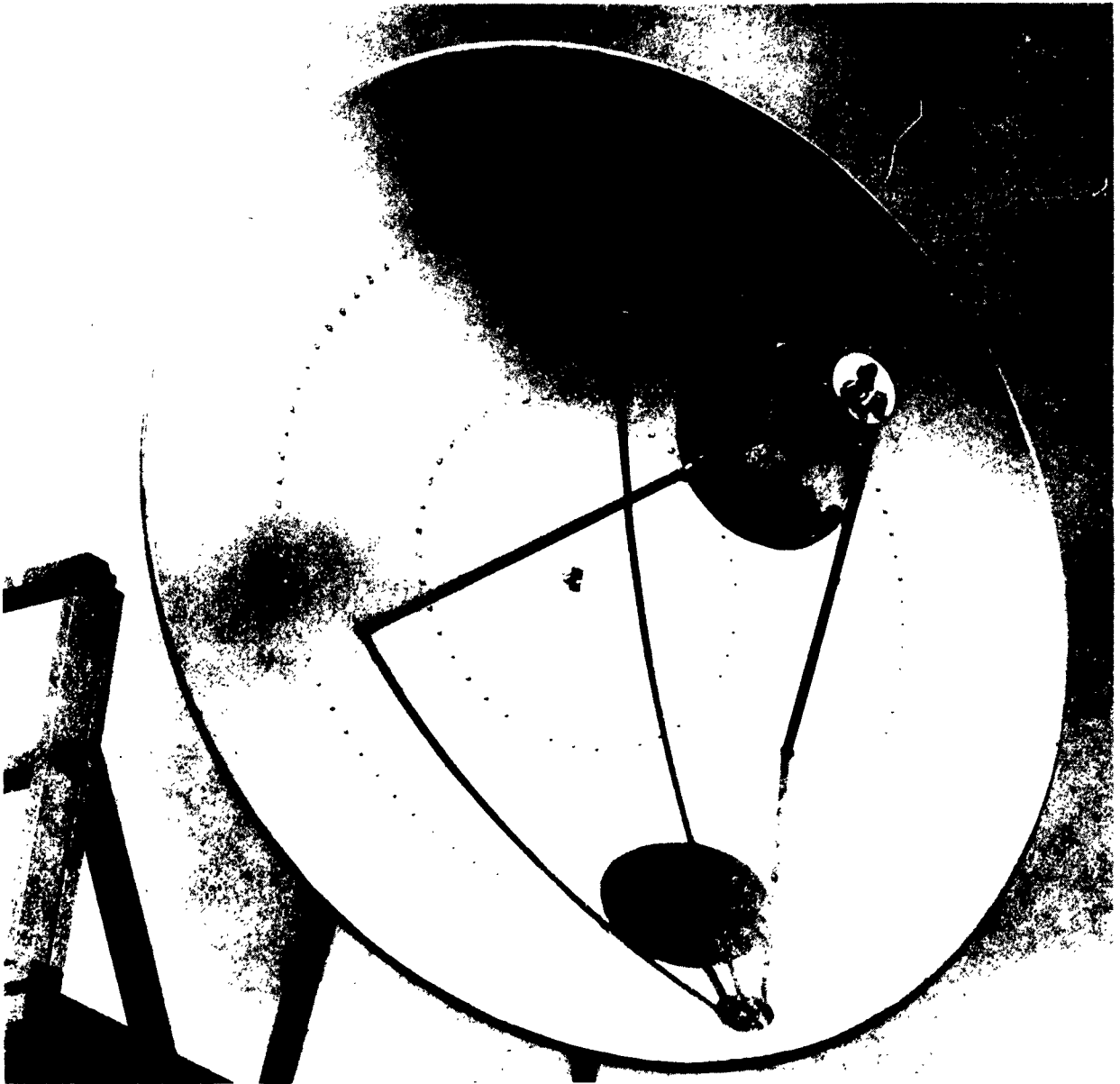


Figure 1. Cassegrain Antenna System

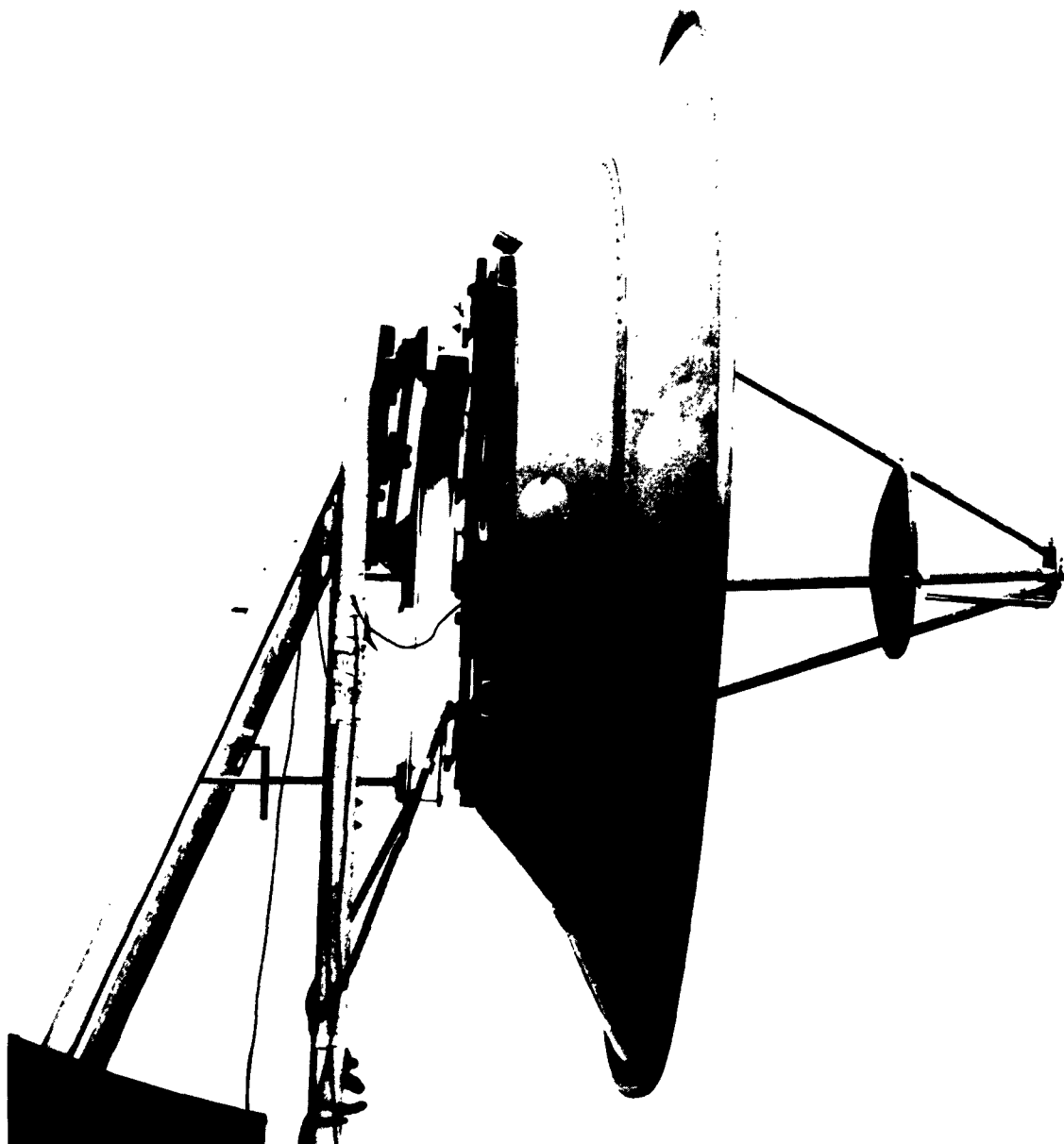


Figure 2. Side View Detail of Cassegrain Antenna System



Figure 3. Field Setup for Taking Measurements



### Section 3. EXPERIMENTAL RESULTS

The  $360^\circ$  patterns showed no lobes past  $30^\circ$  indicating that any back radiation is less than the sensitivity of the receiver. ( $-40$  db from the main lobe). Figures 4 through 8, and 9 through 13 are the  $12^\circ$  and  $60^\circ$  azimuth patterns respectively taken at increasing distances from the antenna assembly. They show that the main lobe tends to become narrow as the distance decreases -- with a bifurcation appearing in the beam whenever  $w$  is an odd multiple of  $\pi$  -- until the Near Zone is reached. In the Near Zone the main lobe again widens but, instead of splitting, appears to peak on axis.

Of considerable interest are the sidelobes appearing at approximately  $17^\circ$  on either side of the main lobe, varying approximately 16 db to 26 db down from the main lobes depending on distance. They are caused by forward spillover of the primary feed around the hyperboloidal subdish.

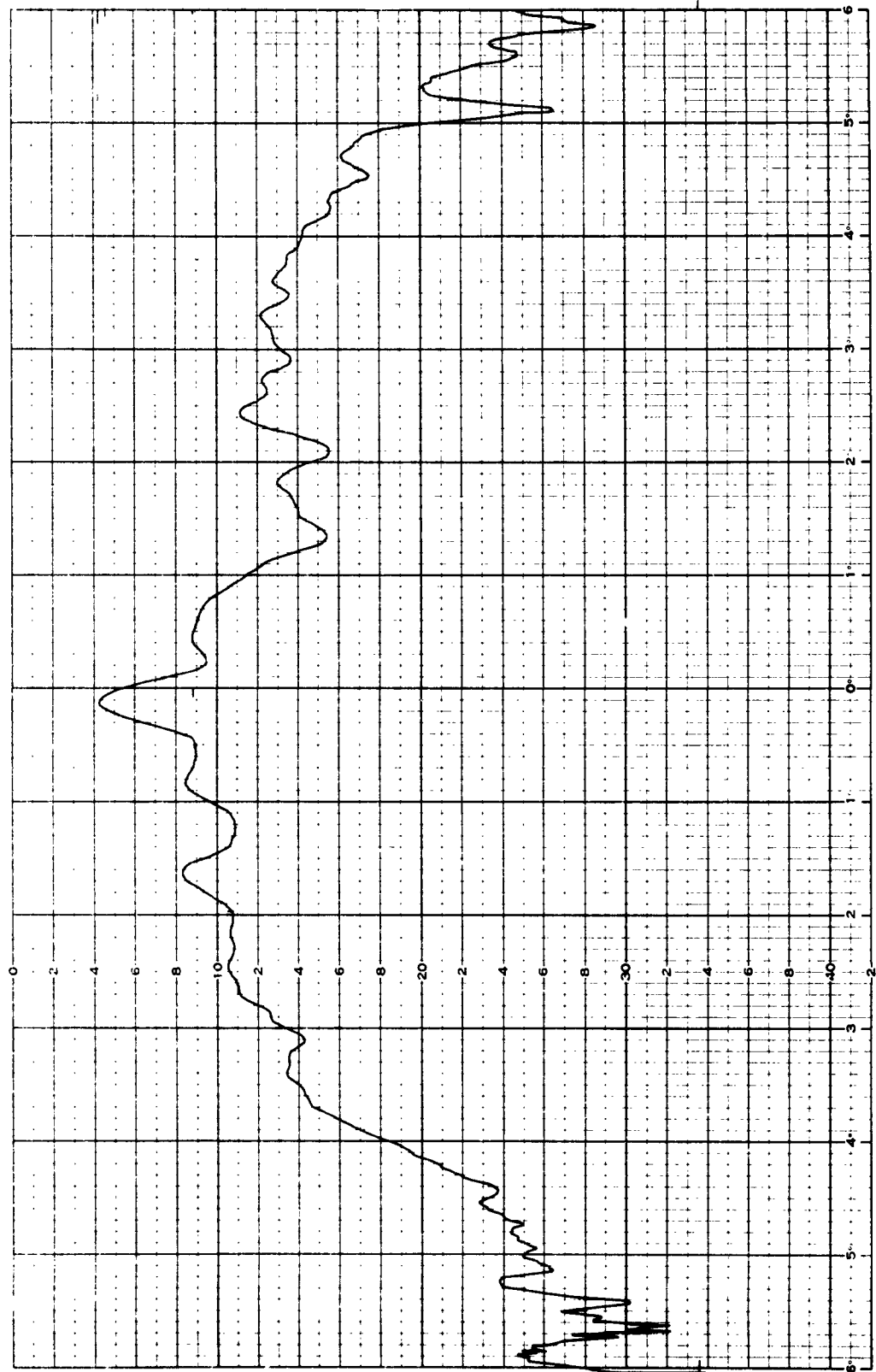


Figure 4.  $w = 68\pi$ ,  $12^\circ$  Azimuth Pattern

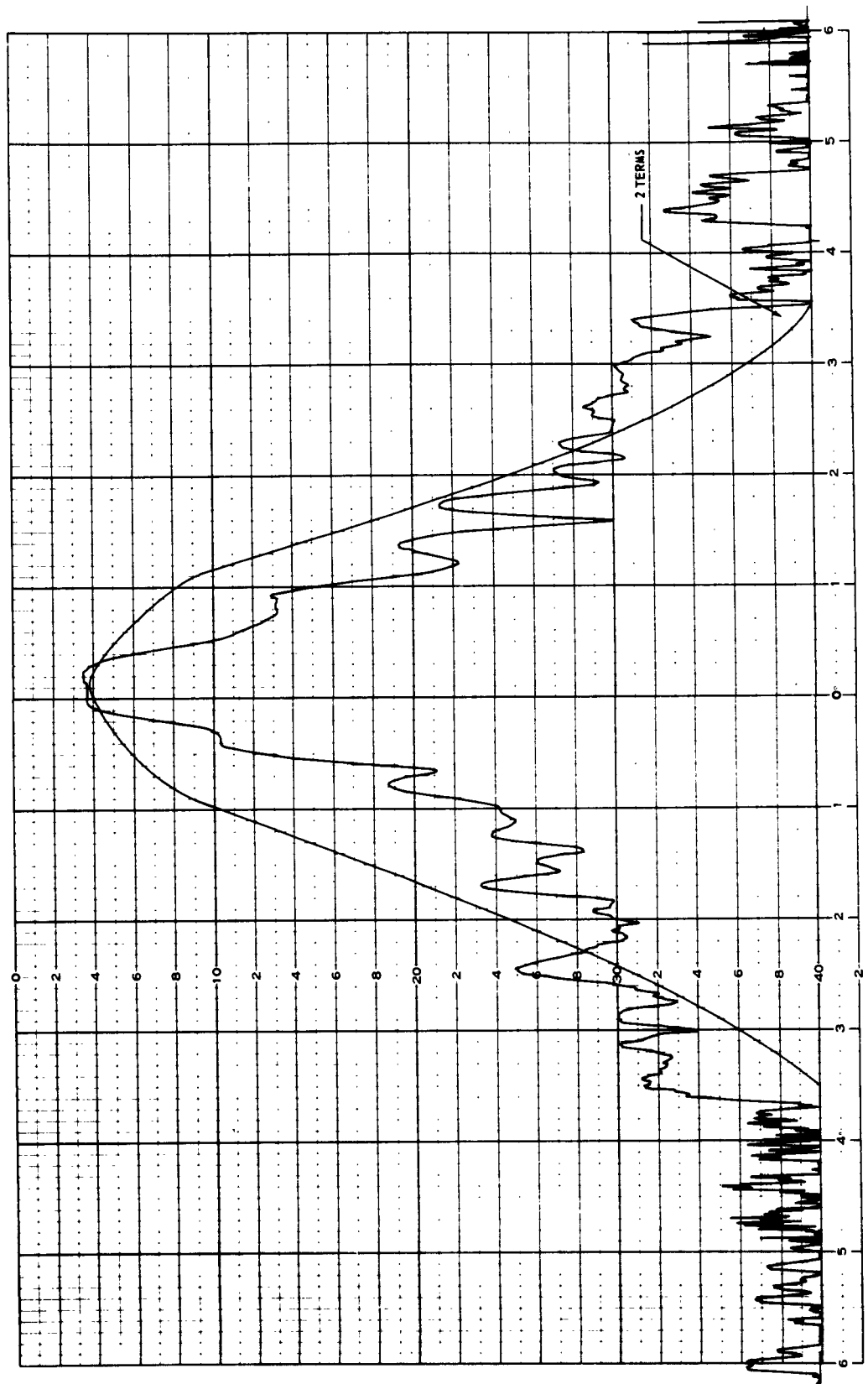


Figure 5.  $w = 34\pi$ ,  $12^\circ$  Azimuth Pattern

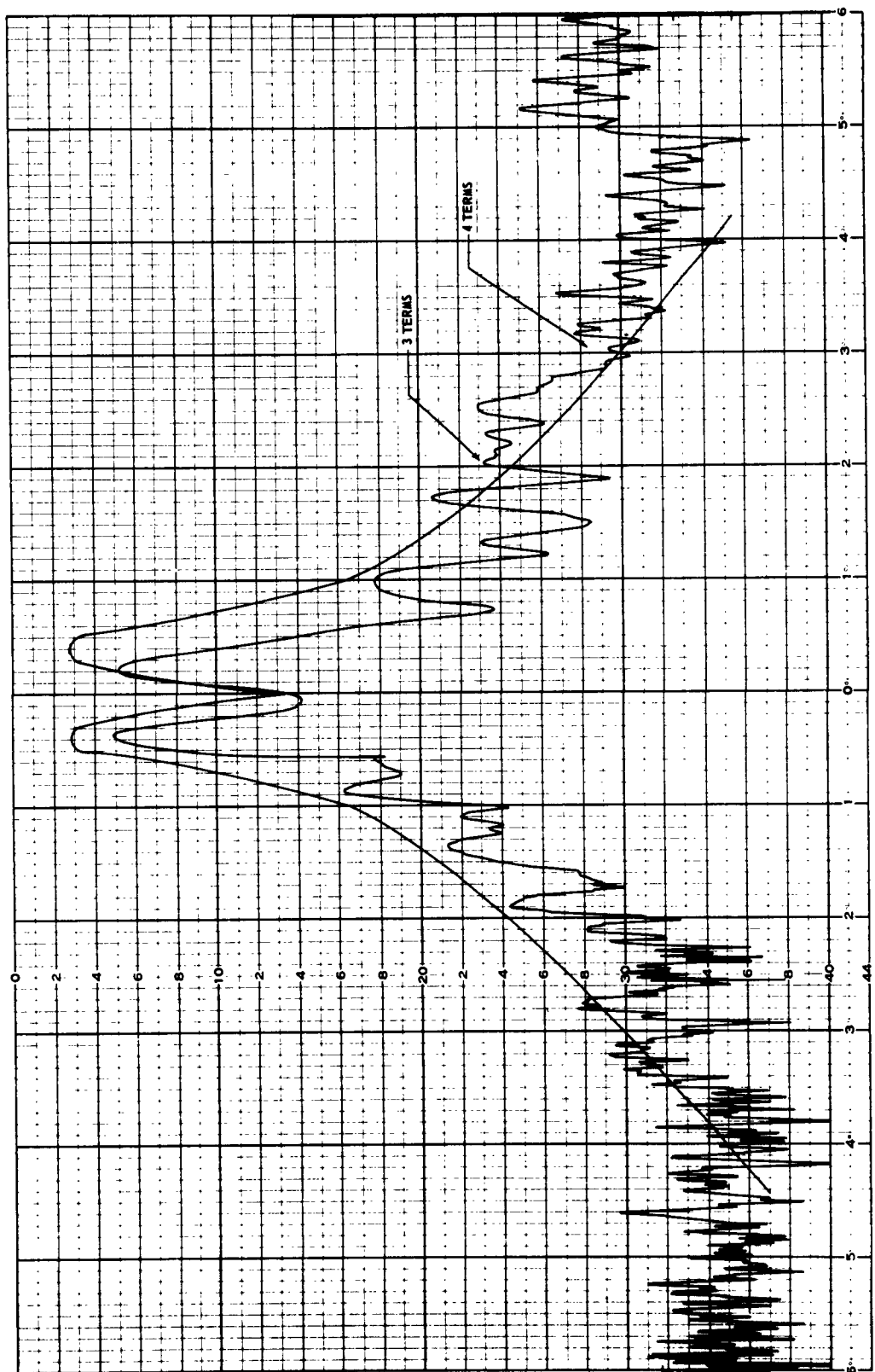


Figure 6.  $w = 33\pi$ , 12° Azimuth Pattern

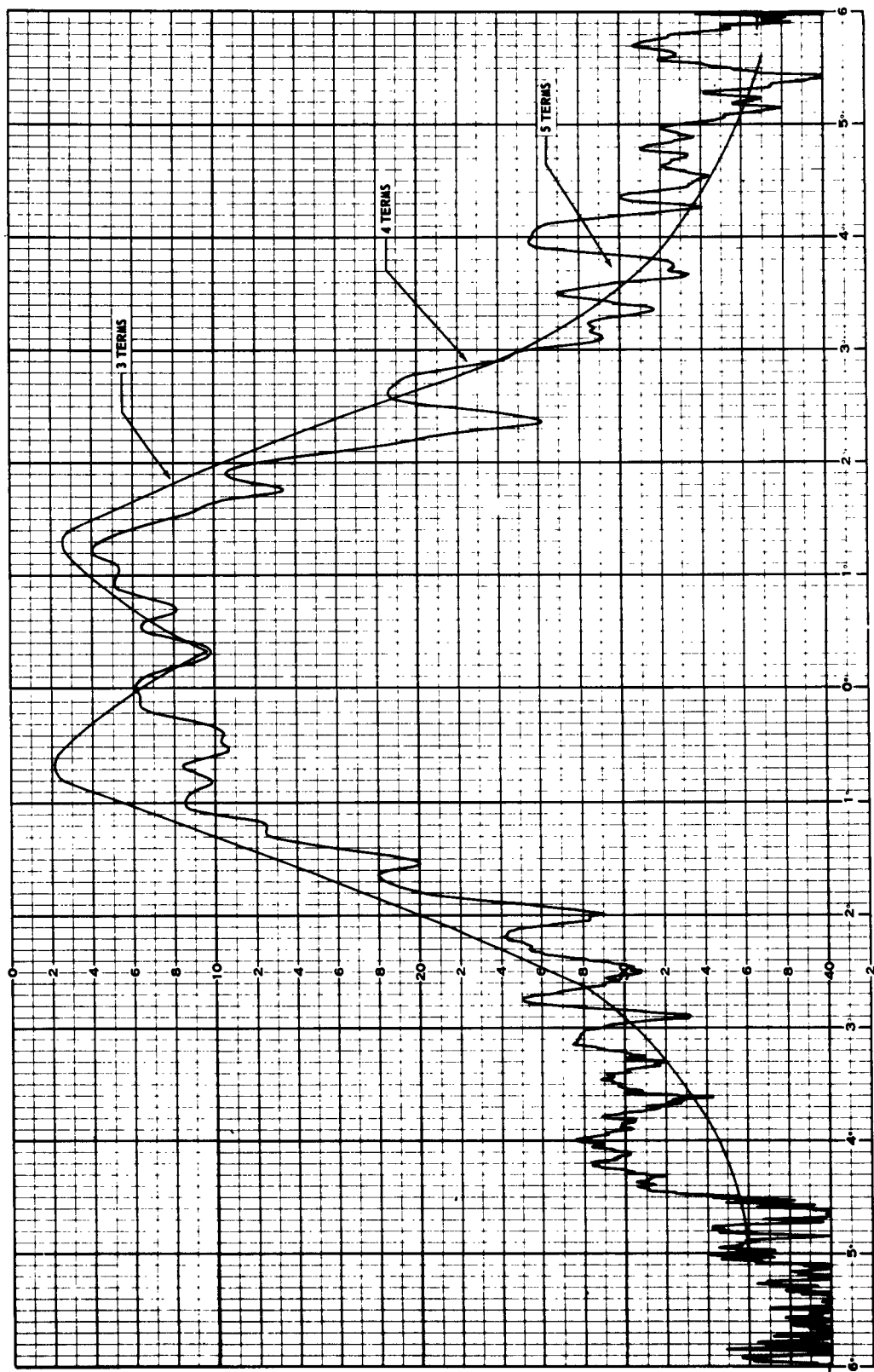


Figure 7.  $w = 17\pi$ ,  $12^\circ$  Azimuth Pattern

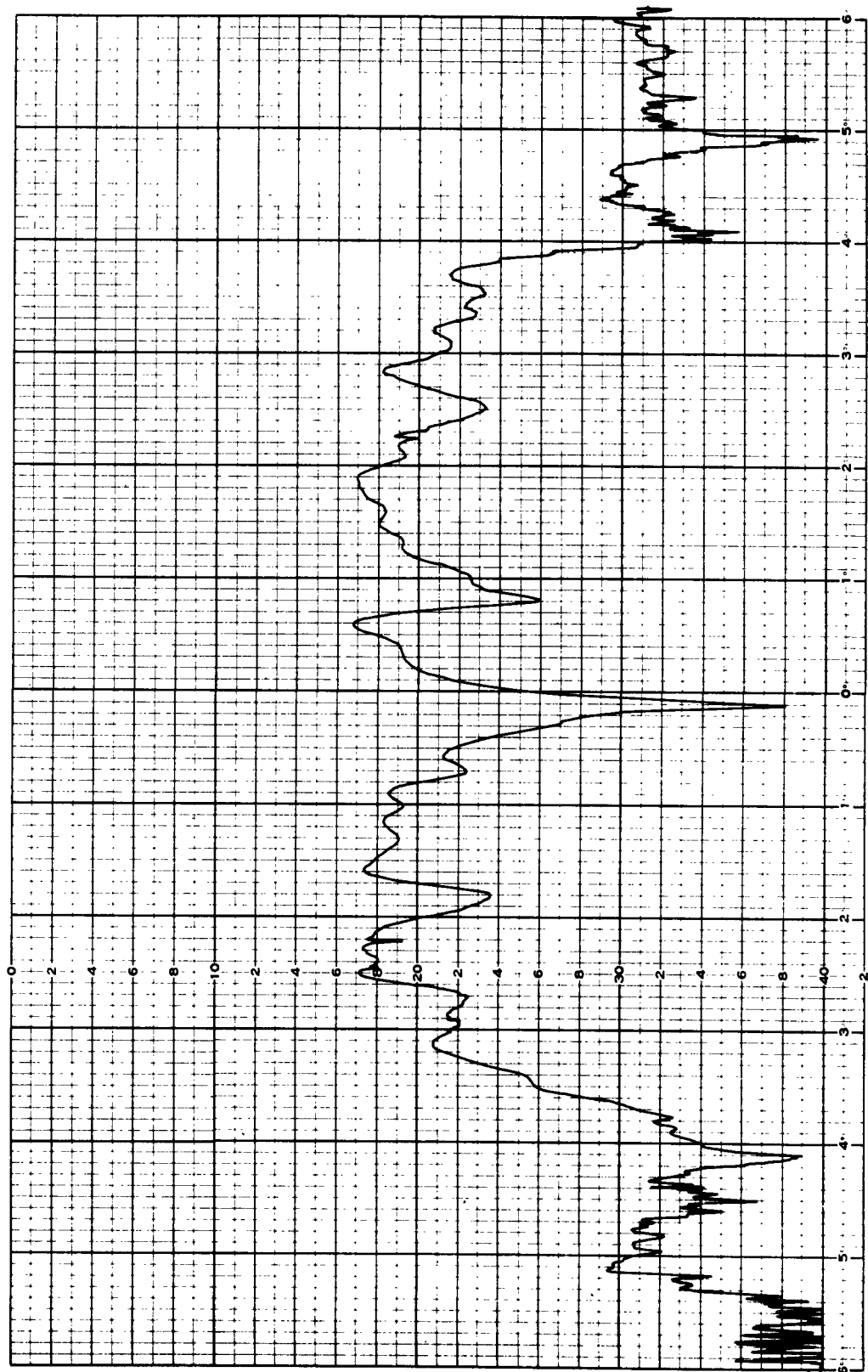


Figure 8.  $w = 3.6\pi$ ,  $12^\circ$  Azimuth Pattern

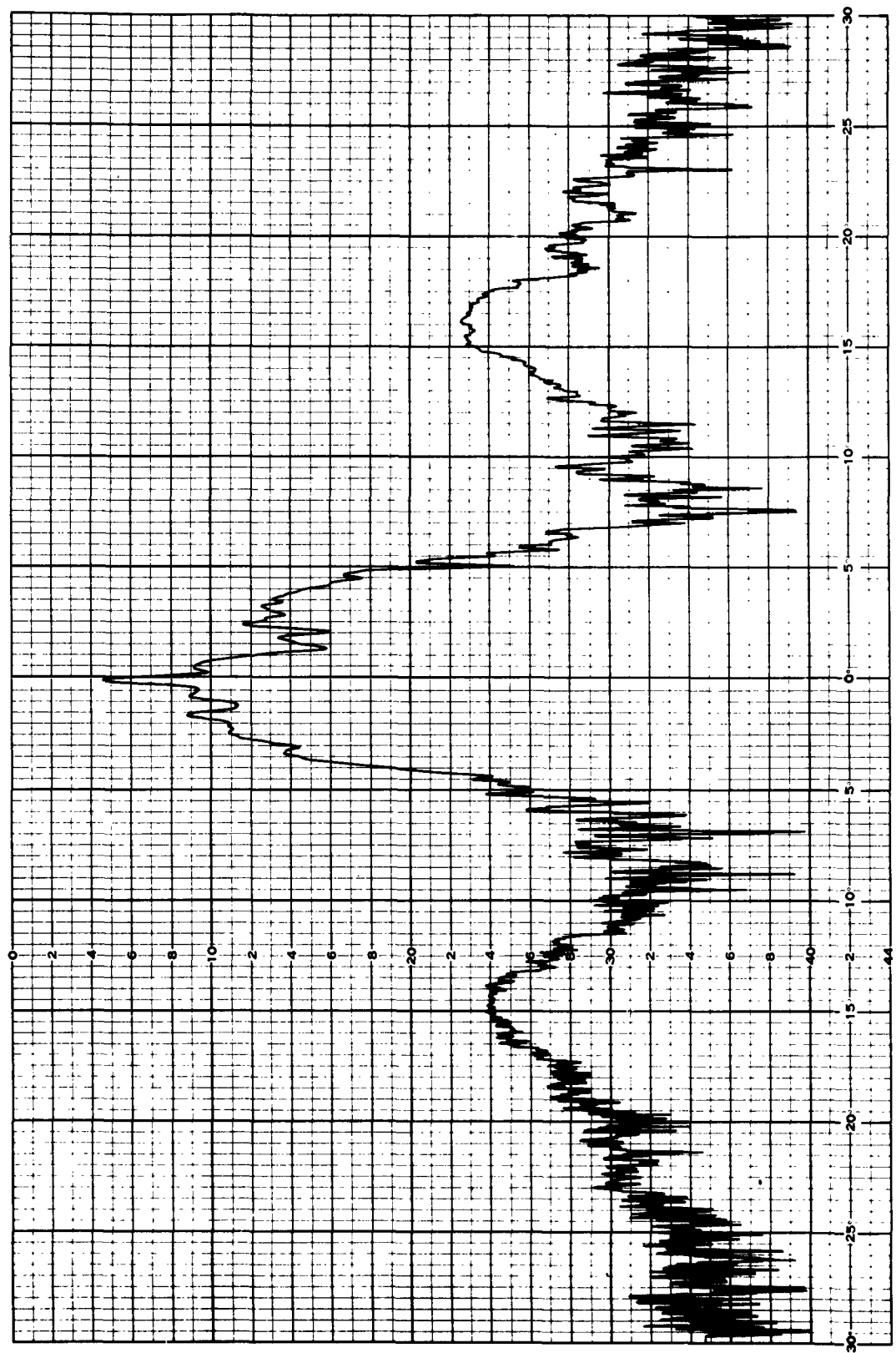


Figure 9.  $w = 68\pi$ ,  $60^\circ$  Azimuth Pattern

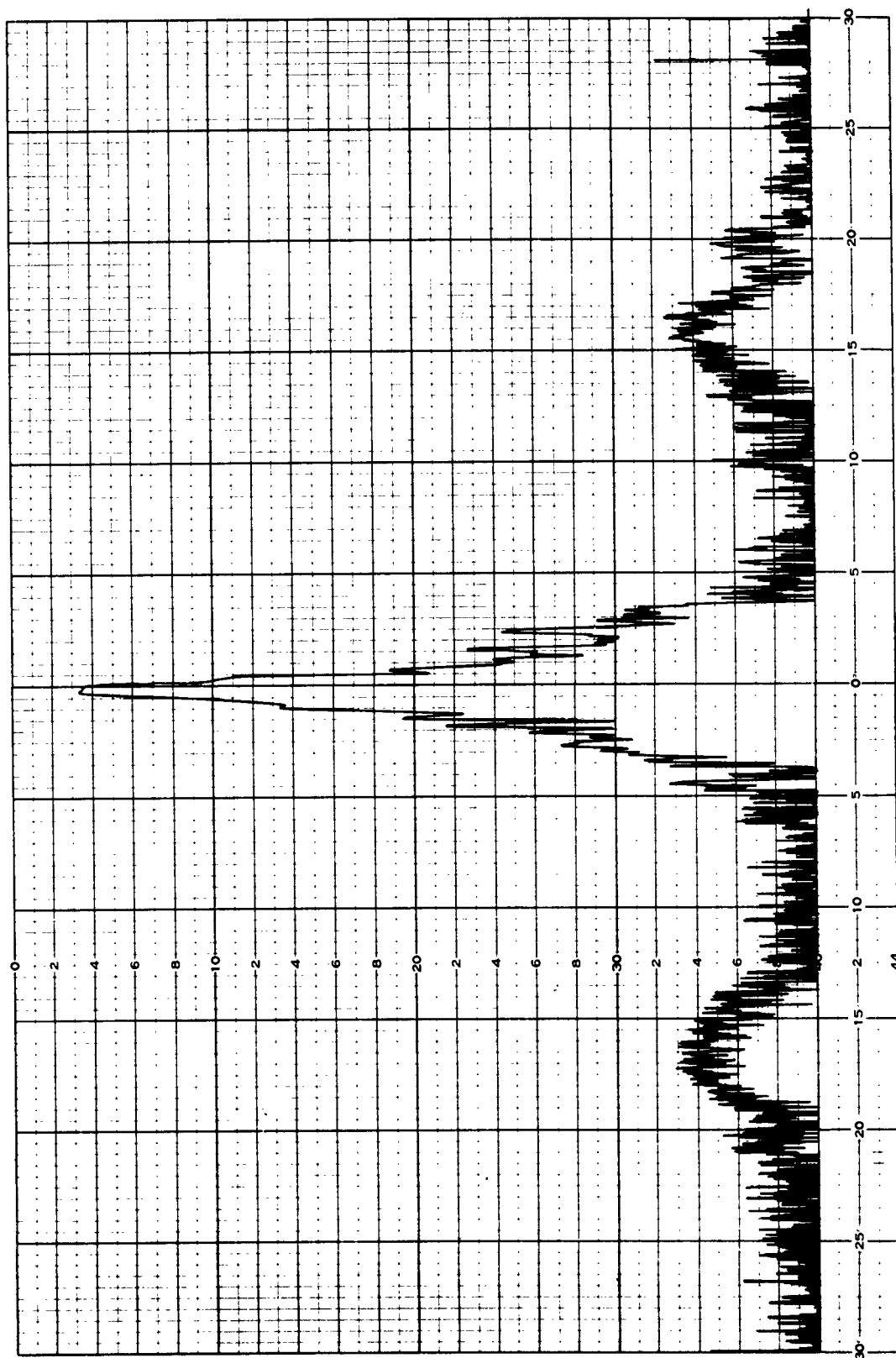


Figure 10.  $w = 34\pi$ , 60° Azimuth Pattern



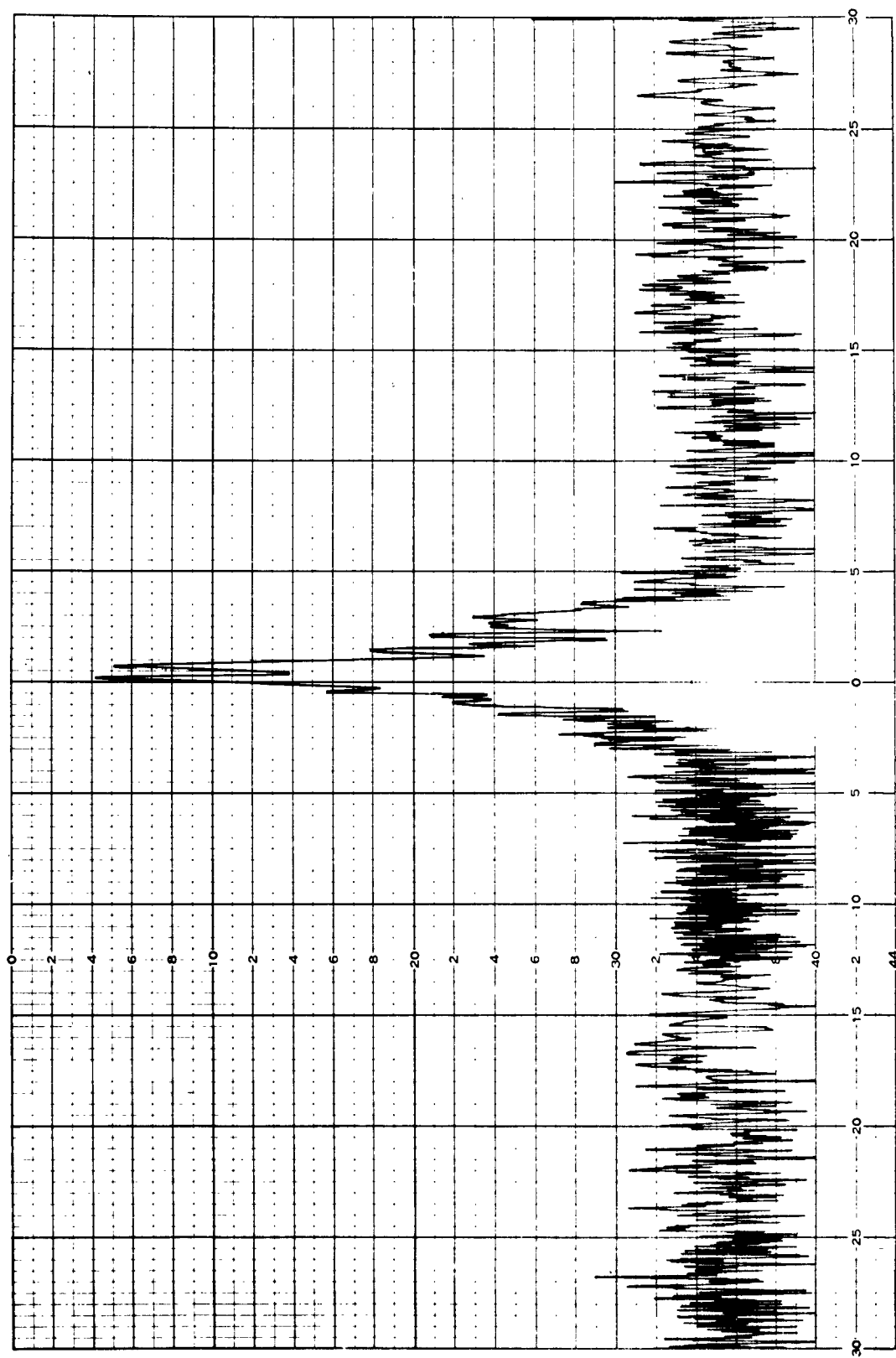


Figure 11.  $w = 33\pi$ ,  $60^\circ$  Azimuth Pattern

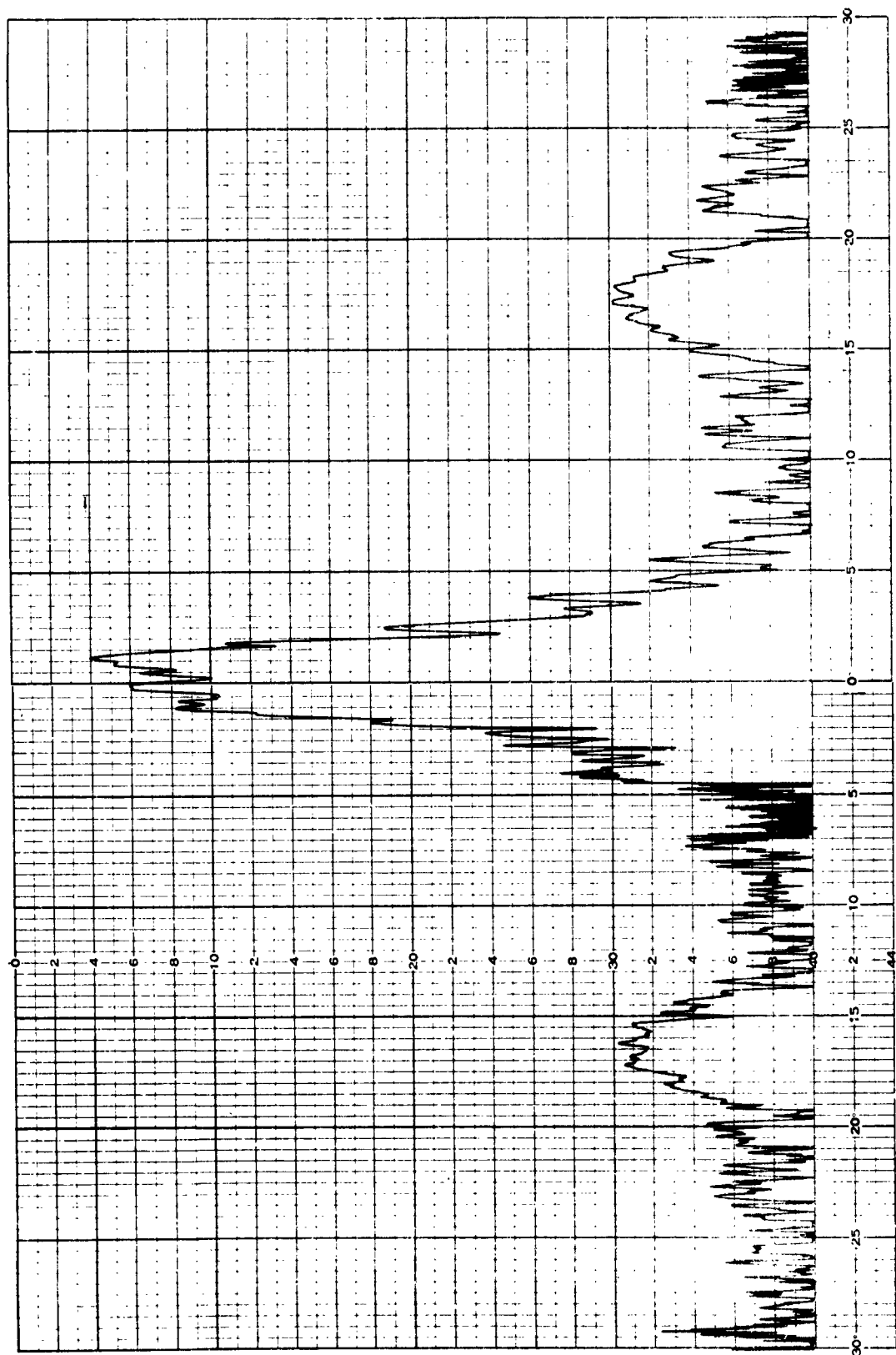


Figure 12.  $w = 17\pi$ ,  $60^\circ$  Azimuth Pattern

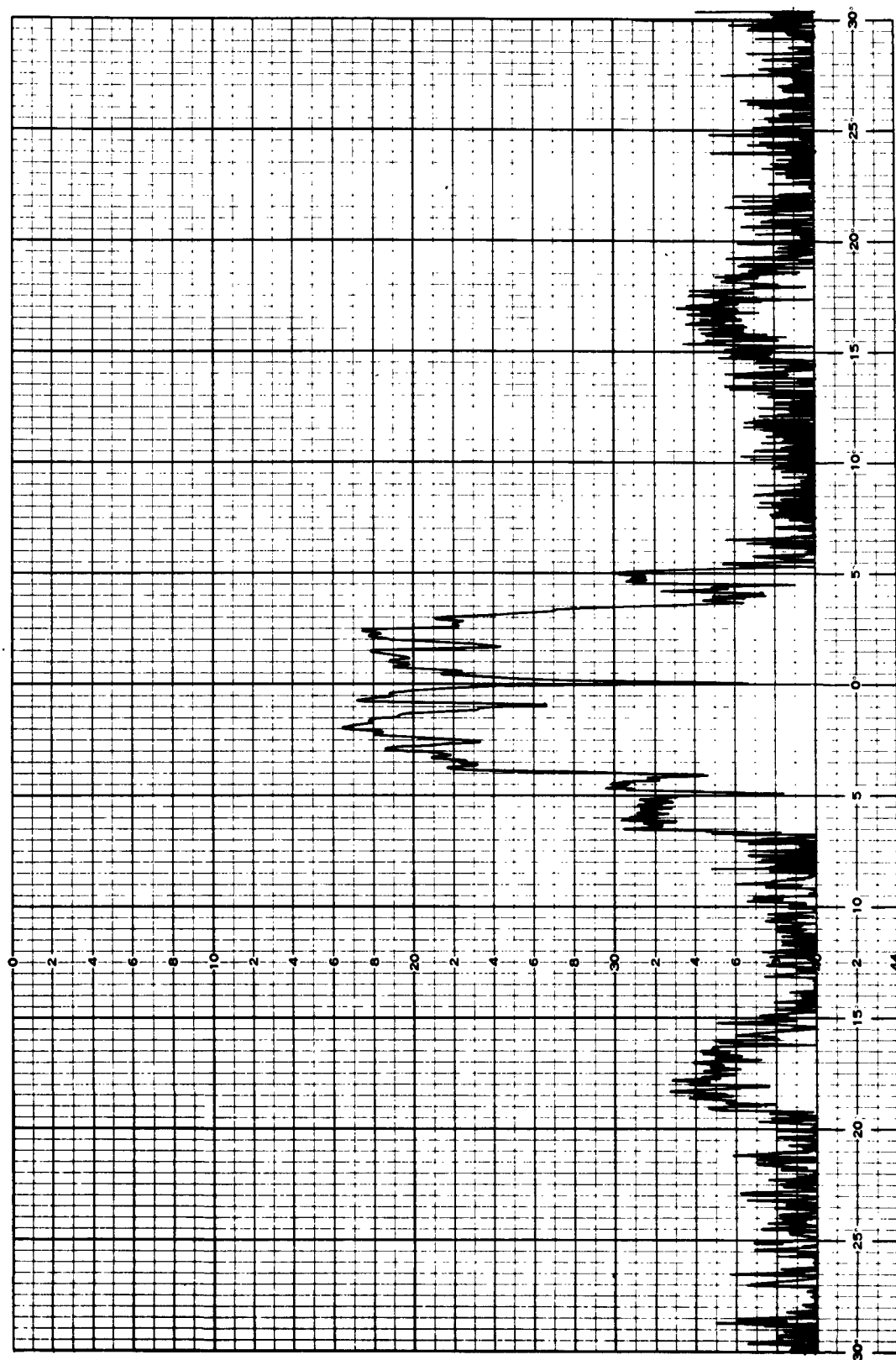


Figure 13.  $w = 3.6\pi$ ,  $60^\circ$  Azimuth Pattern

## Section 4. THEORETICAL INVESTIGATION

The amplitude distribution and power pattern of a circular aperture having the dimensions, aperture illumination taper, and operating frequency of the test antenna were calculated using an "off-axis" field expression for the Fresnel Region derived in terms of the Fresnel integral and Lommel's functions of two variables. The solution for an aperture illumination taper of 10 db using the form  $(1 - \xi^2)^n$  where  $n = 1$ , is that described by Hu.(3) The "on-axis" field was derived in a similar manner using Lommel's functions for a single variable.

### 4.1 THE FRESNEL INTEGRAL OF THE DIFFRACTION FIELD "OFF AXIS"

The diffraction integral for the optical Fresnel region of a circular aperture has been defined by Silver,(4)

$$E = j/2\lambda R \int_0^{2\pi} \int_0^a F(\rho, \theta) e^{-jk r_z} (\cos \theta + \bar{i} \cdot \bar{s}) \rho d\rho d\theta \quad (1)$$

where  $\rho$  and  $\theta$  are in terms of polar coordinates,  $(\bar{i} \cdot \bar{s})$  represents non-uniform phase distribution over the aperture,  $F(\rho, \theta)$  represents the amplitude distribution. The  $r_z$  term retains only the linear and quadratic terms (in  $\rho/R$ ) in the binominal expansion of the phase factor.

Then

$$\begin{aligned} r_z &= \left| R^2 + \rho^2 - 2R\rho \sin \theta \cos(\delta - \beta) \right|^{1/2} \\ &= R - \rho \sin \theta \cos(\delta - \beta) + \rho^2/2R \left| 1 - \sin^2 \theta \cos^2(\delta - \beta) \right| \\ r_z &= R - \rho \sin \theta \sin \beta + \rho^2/2R \cos^2 \theta \end{aligned}$$

For uniform phase and amplitude distribution across the aperture equation (1) may be defined as

$$\mathcal{E} = \frac{j e^{-jkR}}{2\lambda R} \mathcal{F}(\rho, \beta) (1 + \cos \theta) \quad (2)$$

where

$$\mathcal{F}(\rho, \beta) = \int_0^{2\pi} \int_0^a e^{jk(\rho \sin \theta \sin \beta - \rho^2/2R \cos^2 \theta)} \rho d\rho d\beta \quad (3)$$

letting  $\xi = \rho/a$ ,  $\mu = \frac{2\pi a}{\lambda} \sin \theta = ka \sin \theta$ ,  $\rho \sin \theta = \frac{\mu \xi}{k}$

$$\mathcal{F}(\mu, \xi) = a^2 \int_0^{2\pi} \int_0^1 e^{j\mu \xi \sin \beta - jk \frac{a^2 \xi^2}{2R} \cos^2 \theta} \xi d\xi d\beta \quad (4)$$

Integrating over  $\beta$ , letting  $w = \frac{ka^2}{R} = \frac{2\pi a^2}{\lambda R}$

$$\mathcal{F}(\mu, \xi) = 2\pi a^2 \int_0^1 J_0(\mu, \xi) e^{-jk \left( \frac{a^2 \xi^2}{2R} \cos^2 \theta \right)} \xi d\xi \quad (5)$$

Where  $J_0(\mu, \xi)$  is the Bessel function of order zero.

The integral in equation (5) may be expressed as a pair of Lommel functions of two variables.

$$\left| U_v(\mu, w) + j U_{v+1}(\mu, w) \right| = \frac{w^v}{\mu^{v-1}} \int_0^1 J_{v-1}(\mu, \xi) e^{\frac{jw}{2}(1-\xi^2)} \xi^{2v-1} d\xi \quad (6)$$

where  $v = 1$ ,  $w = ka^2/R \cos^2 \theta$

7.

Equation (5) then becomes

$$\mathcal{F}(\mu, \xi) = \frac{2\pi a^2 e^{-jw/2}}{w} \left| U_v(\mu, w) + jU_{v+1}(\mu, w) \right| \quad (7)$$

For non-uniform amplitude illumination of the aperture having a 10 db taper equation (5) has the form when  $\theta$  is small,

$$\mathcal{F}(\mu, \xi)_1 = 2\pi a^2 \int_0^1 (1-\xi^2) J_0(\mu, \xi) e^{-j\frac{w}{2}\xi^2} \xi d\xi \quad (8)$$

Since

$$\frac{\partial}{\partial w} \left[ \frac{U_v(\mu, w)}{w} + \frac{jU_{v+1}(\mu, w)}{w} \right] = \frac{\partial}{\partial w} \left[ \int_0^1 J_{v-1}(\mu, \xi) e^{j(1-\xi^2)\frac{w}{2}} \xi^v d\xi \right] \quad (9)$$

$$= j/2 \int_0^1 (1-\xi^2) J_{v-1} e^{j(1-\xi^2)\frac{w}{2}} \xi^v d\xi$$

$$\mathcal{F}(\mu, \xi)_1 = \frac{4\pi a^2}{j} e^{-j\frac{w}{2}} \frac{\partial}{\partial w} \left[ \frac{U_v(\mu, w)}{w} + j \frac{U_{v+1}(\mu, w)}{w} \right] \quad (10)$$

Then for an amplitude illumination taper of 10 db, equation (2) becomes

$$\mathcal{F}_1 = \frac{j e^{j(\frac{w}{2} - kR)}}{2\lambda R} \mathcal{F}(\mu, \xi)_1 (1 + \cos\theta)$$

$$\mathcal{F}_1 = w e^{j(\frac{w}{2} - kR)} \frac{\partial}{\partial w} \left[ \frac{U_v(\mu, w)}{w} + j \frac{U_{v+1}(\mu, w)}{w} \right] (1 + \cos\theta) \quad (11)$$

#### 4.2 THE FRESNEL INTEGRAL OF THE DIFFRACTION FIELD "ON AXIS"

For the diffraction field on the axis,  $\theta = 0$  and equation (3) reduces to

$$\mathcal{F}(\rho, \beta) = \int_0^{2\pi} \int_0^a e^{-j \frac{k\rho^2}{2R}} \rho d\rho d\beta \quad (12)$$

letting  $\xi = \rho/a$  and integrating over  $\beta$

$$\mathcal{F}(\xi, 0) = 2\pi a^2 \int_0^1 e^{-j \frac{k\xi^2 a^2}{2R}} \xi d\xi \quad (13)$$

The integral in equation (13) may be expressed as a pair of Lommel functions of one variable

$$\left| U_v(w, 0) + j U_{v+1}(w, 0) \right| = \frac{w^v}{2^{v-1} r(v)} \int_0^1 e^{j \frac{w}{2} (1 - \xi^2)} \xi^{2v-1} d\xi \quad (14)$$

where  $v = 1$ ,  $w = \frac{ka^2}{R}$

Equation (13) then becomes

$$\mathcal{F}(\xi, 0) = 2\pi a^2 e^{-j \frac{w}{2}} \frac{\left| U_v(w, 0) + j U_{v+1}(w, 0) \right|}{w} \quad (15)$$

For non-uniform amplitude illumination of the aperture having a 10 db taper equation (13) becomes

$$\mathcal{F}(\xi, 0) = 2\pi a^2 \int_0^1 (1 - \xi^2) e^{-j \frac{w}{2} \xi^2} \xi d\xi \quad (16)$$

Since

$$\begin{aligned} \frac{\partial}{\partial w} \left[ \frac{U_v(w,0)}{w} + j \frac{U_{v+1}(w,0)}{w} \right] &= \frac{\partial}{\partial w} \left[ \int_0^1 e^{j \frac{w}{2} (1 - \xi^2)} \xi^{2v-1} d\xi \right] \\ &= j/2 \int_0^1 (1 - \xi^2) e^{j \frac{w}{2} (1 - \xi^2)} \xi^{2v-1} d\xi \end{aligned}$$

$$\mathcal{F}(\xi, 0) = e^{-j \frac{w}{2}} \frac{4\pi a^2}{j} \frac{\partial}{\partial w} \left[ \frac{U_v(w,0)}{w} + j \frac{U_{v+1}(w,0)}{w} \right] \quad (17)$$

Then for an amplitude illumination taper of 10 db, equation (2) becomes

$$\mathcal{F}_{01} = \frac{j e^{j(\frac{w}{2} - kR)}}{2\lambda R} \mathcal{F}(\xi, 0)$$

$$\mathcal{F}_{01} = w e^{j(\frac{w}{2} - kR)} \frac{\partial}{\partial w} \left[ \frac{U_v(w,0)}{w} + j \frac{U_{v+1}(w,0)}{w} \right] \quad (18)$$



## Section 5. COMPARISON OF THEORETICAL AND EXPERIMENTAL PATTERNS

In computing the theoretical power patterns, the "off-axis" field expressions were normalized with respect to the "on-axis" expression for a given distance and then transformed logarithmically by  $20 \log E_1/E_{01}$  to correspond dimensionally with the experimental data. Hu(3) has plotted field distributions up to a distance where  $w = 2\pi$ , the point of maximum power density on axis, for a circular aperture using dimensions and wavelength such that the curves plotted extend no further off axis than the point  $\mu = 12$  where  $\mu = (2\pi/\lambda) a \sin \theta$ . In doing so he expands the Lommel function, which may be expressed as a power series, to six terms and then differentiates the series term-by-term to obtain the expression for a 10 db taper, in the following manner.

$$\begin{aligned}
 U_1(w, \mu) &= w \frac{J_1(\mu)}{\mu} - w^3 \frac{J_3(\mu)}{\mu^3} + w^5 \frac{J_5(\mu)}{\mu^5} - w^7 \frac{J_7(\mu)}{\mu^7} \\
 &\quad + w^9 \frac{J_9(\mu)}{\mu^9} - w^{11} \frac{J_{11}(\mu)}{\mu^{11}} + \dots \\
 U_2(w, \mu) &= w^2 \frac{J_2(\mu)}{\mu^2} - w^4 \frac{J_4(\mu)}{\mu^4} + w^6 \frac{J_6(\mu)}{\mu^6} - w^8 \frac{J_8(\mu)}{\mu^8} \\
 &\quad + w^{10} \frac{J_{10}(\mu)}{\mu^{10}} - w^{12} \frac{J_{12}(\mu)}{\mu^{12}} + \dots \\
 \frac{\partial}{\partial w} \left[ \frac{U_1(w, \mu)}{w} \right] &= 0 - 2w \frac{J_3(\mu)}{\mu^3} + 4w^3 \frac{J_5(\mu)}{\mu^5} - 6w^5 \frac{J_7(\mu)}{\mu^7} \\
 &\quad + 8w^7 \frac{J_9(\mu)}{\mu^9} - 10w^9 \frac{J_{11}(\mu)}{\mu^{11}} \\
 \frac{\partial}{\partial w} \left[ \frac{U_2(w, \mu)}{w} \right] &= \frac{J_2(\mu)}{\mu^2} - 3w^2 \frac{J_4(\mu)}{\mu^4} + 5w^4 \frac{J_6(\mu)}{\mu^6} - 7w^6 \frac{J_8(\mu)}{\mu^8} \\
 &\quad + 9w^8 \frac{J_{10}(\mu)}{\mu^{10}} - 11w^{10} \frac{J_{12}(\mu)}{\mu^{12}}
 \end{aligned}$$

The "on-axis" expression of Lommel functions of one variable when expanded as a power series is recognized as being trigonometric in form

$$\text{where } U_1(w,0) = w/2 - \frac{(w/2)^3}{3!} + \frac{(w/2)^5}{5!} - \dots = \sin w/2$$

$$U_2(w,0) = -\frac{(w/2)^2}{2!} + \frac{(w/2)^4}{4!} - \frac{(w/2)^6}{6!} + \dots = \cos \frac{w}{2} - 1$$

$$= 2 \sin^2 (w/4)$$

$$\frac{\partial}{\partial w} \left[ \frac{U_1(w,0)}{w} \right] = \left[ \frac{\cos w/2}{2w} - \frac{\sin w/2}{w^2} \right]$$

$$\frac{\partial}{\partial w} \left[ \frac{U_2(w,0)}{w} \right] = \left[ \frac{\sin w/4 \cos w/4}{w} - \frac{2 \sin^2 w/4}{w^2} \right]$$

The expansion of the Lommel function to six terms as employed by Hu in the "off-axis" expression, while an excellent approximation at distances from the  $10\lambda$  aperture where  $\omega \leq 2\pi$ , would not be adequate for distances close to the same aperture where the magnitude of  $\omega$  is as large as described in the experimental work of this paper. Thus for values of  $\omega$  large with respect to  $\mu$ , an asymptotic expansion of the form

$$U_n(\omega, \mu) \sim \cos \left( \frac{\omega}{2} + \frac{\mu^2}{2\omega} - \frac{n\pi}{2} \right) + \sum_{m=0}^{\infty} (-)^m (\mu/\omega)^{2m-n+2} J_{n-2-2m}(\mu)$$

would be more appropriate for the same number of terms. <sup>(4)</sup>

Fortunately, however, (with respect to ease of numerical analysis) the major portion of the field in the experimental patterns of this paper extend only several degrees from the beam axis. Yet the large aperture ( $350\lambda$ ) employed causes the magnitude of  $\mu$  to become exceedingly large within the range of analysis. Thus, at a point less than  $1/2$  degree off axis the ratio of  $\omega$  to  $\mu$  is such that the expression for  $U_{(w,\mu)}$  may be approximated using only a few terms of the Neumann type series and as the magnitude of  $\omega$  decreases the field may be determined more closely to the axis.

## Section 6      CONCLUSIONS AND RECOMMENDATIONS

The use of Lommel functions in evaluating the Fresnel Region field distribution near a circular aperture is an excellent approach if care is exercised in selecting the number of terms used in the series expansion, and the field distribution of any Cassegrain antenna having an aperture diameter of  $350\lambda$  may be predicted using the number of terms shown in the figures referenced above for normalized distances of  $w = 33\pi$ ,  $34\pi$  and  $17\pi$ . Further experimental investigation of the number of terms needed for various aperture diameters and distances should yield a general mathematical model for prediction of Fresnel Region distributions. The principal defects of the Cassegrain antenna in the Near field and Fresnel Region, with respect to interference, are poor forward spillover properties and broadening of the main lobe by as much as 20 times the far field 3 db beamwidth of  $(0.166^\circ)$ . Of the two, the forward spillover is probably the more serious for it not only increases the probability of on-site mutual interference but also the antenna noise temperature, and decreases the aperture efficiency. The pattern created by the forward spillover is dependent on the aperture dimensions of the primary feed and the blocking subdish, and may therefore be considered as essentially a far field pattern. By estimating the antenna gain in the direction of the forward spillover from experimental patterns and using the Friis transmission formula where

$$\frac{P_r}{P_t} = \frac{G_T G_R \lambda^2}{16\pi^2 z^2}$$

the mutual coupling between two identical Cassegrain antennas facing each other  $17^\circ$  off axis may be easily predicted.

$w$	$P_r/P_t$ (-db)
$68\pi$	57
$34\pi$	73
$17\pi$	88
$17\pi$	75
$36\pi$	95

It has been suggested by Professor C. M. Salati,\* that the edges of the subreflector in a two-reflector system be modified to reduce the forward spillover by use of absorbing material, serrating the edges, or some other method of disrupting the edge currents. A method which met with considerable success for a large Cassegrain system has been described by P. D. Potter(6) where, using a conical extension flange having a diameter of 14 inches and flange angle of  $18.4^\circ$  at the outer edge of a hyperboloidal subreflector having a diameter of 9.6 inches and a half aperture angle of  $60^\circ$ , spillover was reduced by a factor of 2.

Investigation of the forward spillover properties of various types of two-reflector systems would appear to be worthwhile. For example, the Schwarzschild system, which differs from the Cassegrain in that it employs a subdish which has a transcendental curve as opposed to a conic section such as a hyperbola, has been indicated by White and Desize(7) to have, theoretically, better off-axis beam characteristics than the Cassegrain with reduced primary coma effects and the capability of producing extremely narrow beams of moderate scan angles.

When the antenna design parameters, placement and tracking configurations of the proposed system become more definite, the use of scale modeling as a tool for specific predictions of on-site susceptibility to interference is highly recommended. In considering the interference problem as concerned with propagation in general, it is apparent that scale modeling is an inexpensive method for verifying and determining the appropriateness of various theoretical mathematical models.

---

\* Conversation at Univ. of Penna., March 1962

### Acknowledgements

Calculations - S. Lim; Measurements - E. Burnham, J. Fuchs

### Bibliography

- (1) Private Communication from General Electric Company, Syracuse, New York. (December 1961) Based on study by G. E. of Global Passive Satellite Communication for RADC.
- (2) A. F. Kay, "Near Field Gain of Aperture Antennas," IRE Trans. Vol. AP-8 November 1960.
- (3) Ming-Kuai Hu, "Study of Near Zone Fields of Large Aperture Antennas," Final Report, Part 2 AF30(602)-928, ASTIA AD-13190, 1957.
- (4) G. N. Watson, "A Treatise on the Theory of Bessel Functions," Cambridge at The University Press, 1952, p 550.
- (5) S. Silver, "Microwave Antenna Theory and Design," RAD. LAB. Series Vol. 12, McGraw-Hill Book Co., 1949.
- (6) P. D. Potter, "A Simple Beamshaping Device for Cassegrainian Antennas," NASA Contract #NAS 7-100, Tech. Report #32-214, JPL Cal. Inst. Technology, 1962.
- (7) W. D. White, L. K. Desize, "Scanning Characteristics of Two Reflector Antenna Systems," Airborne Instruments Lab., IRE National Convention, 1962.
- (8) A. Krinitz, "Radio Frequency Interference in Digital Two-Phase Coherent Communications Systems," RADC-TDR-62-360, Volume IV, Contract AF30(602)-2528, Melpar, Inc.
- (9) David S. White, "Parametric Amplifier Interference Susceptability Study," RADC-TN-62-360, Volume III, Contract AF30(602)-2528, Melpar, Inc.
- (10) Richard W. Chittenden, "Radar Interference Levels at Satellite Communications Terminals," (Sec. Rept.) RADC-TDR-62-360, Volume I, Contract AF30(602)-2528, Melpar, Inc.
- (11) "Long Range Communications Interference Study." Final Report RADC-TDR-62-411, Contract AF30(602)-2528, Melpar, Inc.